

Original citation:

Kampert, Erik, Jennings, P. A. (Paul A.) and Higgins, Matthew D. (2018) Investigating the V2V millimeter-wave channel near a vehicular headlight in an engine bay. IEEE Communications Letters . doi:10.1109/LCOMM.2018.2829181

Permanent WRAP URL:

<http://wrap.warwick.ac.uk/101994>

Copyright and reuse:

The Warwick Research Archive Portal (WRAP) makes this work by researchers of the University of Warwick available open access under the following conditions. Copyright © and all moral rights to the version of the paper presented here belong to the individual author(s) and/or other copyright owners. To the extent reasonable and practicable the material made available in WRAP has been checked for eligibility before being made available.

Copies of full items can be used for personal research or study, educational, or not-for profit purposes without prior permission or charge. Provided that the authors, title and full bibliographic details are credited, a hyperlink and/or URL is given for the original metadata page and the content is not changed in any way.

Publisher's statement:

© 2018 IEEE. Personal use of this material is permitted. Permission from IEEE must be obtained for all other uses, in any current or future media, including reprinting /republishing this material for advertising or promotional purposes, creating new collective works, for resale or redistribution to servers or lists, or reuse of any copyrighted component of this work in other works.

A note on versions:

The version presented here may differ from the published version or, version of record, if you wish to cite this item you are advised to consult the publisher's version. Please see the 'permanent WRAP url' above for details on accessing the published version and note that access may require a subscription.

For more information, please contact the WRAP Team at: wrap@warwick.ac.uk

Investigating the V2V Millimeter-Wave Channel near a Vehicular Headlight in an Engine Bay

Erik Kampert, Paul A. Jennings, Matthew D. Higgins, *Senior Member, IEEE*

Abstract— In this Letter, the first public millimeter wave channel measurements near a vehicular headlight in an engine bay are presented, providing detailed information about the typical excess loss and root mean square delay spread that are experienced in this exemplary V2V communication channel, providing at least 140° field of view. The measurements cover a broad frequency spectrum, ranging from bands considered for future general wireless access to those that are specifically considered for automotive radar applications. The results show that, unless blocked by the vehicle's coachwork, typical excess loss is at least 10 dB, typically 20 dB, and a maximum delay spread of 4 ns is observed. Through the provision of these new real-world measurements, this Letter contributes further to the community by accelerating the development of high-fidelity channel models.

Index Terms— Channel modeling, millimeter wave (mmWave), vehicular communication, V2V, V2X.

I. INTRODUCTION

CONNECTED and autonomous vehicles (CAVs) will depend on fast and reliable vehicle-to-vehicle (V2V) and vehicle-to-everything (V2X) telecommunication, as they have to rely not only on information from their own sensors, but also on that of other vehicles and their environment. This poses significant challenges to the underlying communication system, as information must reliably reach its destination within a short period, beyond what current wireless technologies can provide. In addition, the high data rates necessary for exchange of massive amounts of raw sensor data are not yet supported by current technologies either. 5G, the fifth generation of mobile communication technology, holds promise of improved performance in terms of reduced latency, increased reliability, and higher throughput under higher mobility and connection densities. Moreover, the use of millimeter waves (mmWave) as carriers enables access to the required larger bandwidths [1] [2].

The biggest challenge for the use of mmWave carrier frequencies (CFs) is the high propagation path loss and susceptibility to blockage by building materials. Hence, before implementing mmWave technology into vehicles, it is crucial to understand such large-scale fading parameters and be able to represent the channel conditions accurately in realistic channel models. Complementary to this, multipath components (MPCs) due to in-vehicle mmWave reflections need to be further understood and described in terms of small-scale fading

parameters. Knowledge about the channel conditions is crucial for increasing the efficiency of multiple access techniques, with channel estimation, beamforming and handover depending critically on the channel dynamics. To achieve this level of understanding, detailed vehicular channel measurements need to be performed, covering realistic scenarios and RF technology deployment, addressing industrial and academic challenges.

The channel measurements near a vehicular headlight that are presented in this Letter represent a V2V mmWave communication channel, capable of exchanging large amounts of vehicular sensor data. Our results provide detailed information on the typical excess loss (EL) and root mean square delay spread (RMS-DS), encountered in this scenario.

II. BACKGROUND

The last decade has shown both increased industrial interest and additional focus from academia into research on mmWave applications for vehicular communications, after the potential and necessity of increased data exchange rates and reduced end-to-end latencies for automotive applications had become clear [3]. Because of the ongoing development of international telecommunication standards [4], e.g. by the Third Generation Partnership Project (3GPP), as well as the continuing evolution of mmWave antennas and proposed 5G waveforms, a substantial risk exists to perform vehicular scenario channel measurement research that is superfluous or outdated. Moreover, due to the challenging nature of these campaigns, and the costly investment in the required equipment, only a limited amount of such studies has been reported. The mm-Wave Group at the Fraunhofer Heinrich Hertz Institute in Berlin, Germany has carried out important experimental vehicular communication work, although its studies focus on the IEEE 802.11p standard operated at 5.9 GHz, well below the millimeter band. Among others, in V2V scenarios ranging from highway, to urban, to tunnel convoy [5], as well as at vehicular urban intersections [6] discrete MPCs, their correlation and their dynamics in terms of lifetime, distribution of excess delay and relative Doppler frequency are identified and characterized.

As mentioned in [5], a distinctive characteristic of vehicular communication channels is the position of the antennas. For practical reasons, the antennas in that study were positioned on the car's roof and behind the front windscreen, however, the

This work was supported in part by the WMG centre High Value Manufacturing Catapult, University of Warwick, Coventry, U.K. The experimental equipment was supported in part by EPSRC through the UK-RAS network. Data presented in this paper are available at <http://wrap.warwick.ac.uk/99592/>.

E. Kampert, P. A. Jennings and M. D. Higgins are with WMG, University of Warwick, Coventry CV4 7AL, U.K. (e-mail: e.kampert@warwick.ac.uk; paul.jennings@warwick.ac.uk; m.higgins@warwick.ac.uk).

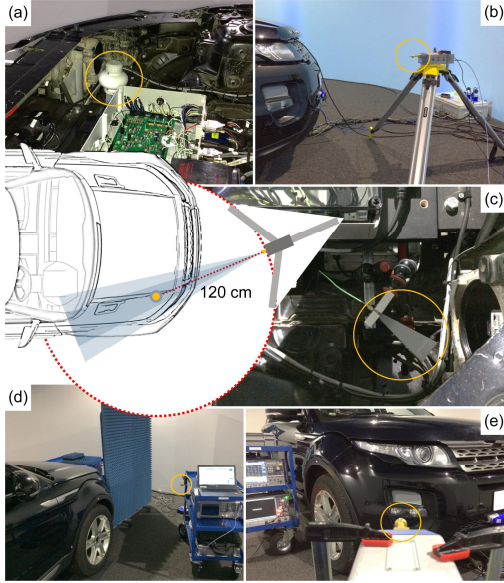


Fig. 1. Photos of the engine bay channel measurements with the aligned TX/RX antenna pair 1 at chosen locations shown in (a) and (d), and pair 2 boresight aligned in various orientations displayed in (b), (c) and (e) (antennas encircled). The central drawing displays the location of RX depicted with a dot, the circular path on which the TX antennas are positioned, and the half-power beam widths of both TX overlaid in grey (light grey 20° , dark grey 10°). automotive industry currently prefers to incorporate antennas in the coachwork, e.g. inside the engine bay. Although to some extent vehicle-specific, the added value provided by this Letter is in understanding the impact of the real antenna environment on the vehicular communication channel, which is substantial and timely given the development pace of 3GPP standards. General knowledge on typical path loss and the presence of MPCs in such environments can be leveraged to refine existing V2V and V2X channel models. Hence, our work presented here, focuses on mmWave channel sounding near a vehicular headlight inside an engine bay. This represents an actual antenna deployment position, which is technically complementary and beneficial, and, because of its corner position, also allowing for V2V communication with adjacent vehicles. In work by Demir *et al.*, an ultra-wideband channel model for an engine compartment has been developed, with a focus on omnidirectional antennas in the frequency range from 3.1 to 10.6 GHz, to be used in an intravehicular wireless sensor network [7]. The maximum measured EL for this frequency range and environment is 6.3 dB, and the MPCs are detected as clusters, which are interpreted in terms of their amplitude and decay rate, and do not vary significantly with local antenna environment. In their study, neither communication with antennas outside the engine bay are considered, nor are mmWave frequencies included, which we cover in this work.

The frequency band from 5.850 to 5.925 GHz is the currently regulated spectrum for V2V in intelligent transport systems (ITS) and dedicated short-range communications (DSRC). This provides sufficient bandwidth for instant road safety applications; however, with increasing numbers and diversity of vehicular sensors, and the unlocked potential of intervehicle raw sensor data sharing, larger bandwidths are required. Latest developments in spectrum allocation foresee sharing parts of the mmWave spectrum that is currently being studied for

International Mobile Telecommunications, as specified in WRC-15 Resolution 238 [8], with other wireless communication users. More specifically, the automotive short and long-range radar bands, ranging from 21.65 to 26.65 GHz and from 77 to 81 GHz, are likely candidates for a combined use with V2X applications. Not least because this would facilitate the use of a single device for both sensing and communication, which is along the progress path of automotive sensor fusion [9]. In order to extend the applicability of our research outcome beyond the vehicular communications domain, seven CFs of [8] were studied during our measurement campaign, namely 25.9; 32.6; 38.5; 62; 68; 74 and 84 GHz. Beyond providing a better understanding of the V2V engine bay channel, our results contribute valuable information to automotive radar applications, which similarly suffer from reduced signal quality due to path loss and delay spread.

III. EXPERIMENTAL DETAILS

The experiment, described here, was conducted in order to understand the implications of the demanding environment in which mmWave antennas for vehicular communications will be placed. Both an omnidirectional antenna and a directional horn antenna (RX) were alternately positioned in an engine bay, near the right vehicular headlight as shown in Fig. 1. The transmitting directional horn antenna (TX) was placed at equal height, in 10° steps, on a circular path with a radius of 120 cm around the RX, and manually boresight aligned with RX. The omnidirectional antenna allowed for the detection of possible MPCs in the engine bay, whereas the horn antenna provided a realistic scenario for directional, vehicular antenna deployment.

In order to perform channel measurements in the full range of mmWave frequencies, globally viable for 5G, two TX/RX antenna pairs were used. Pair 1 consisted of a double ridged guide horn antenna with a typical gain of 20 dBi and a half-power beam width (HPBW) of 20° for frequencies between 24 and 40 GHz, and an ultra-wideband omnidirectional antenna with a typical gain of 6 dBi and an elevation HPBW of 20° for the same frequency range. Pair 2 consisted of two waveguide horn antennas for the frequency range from 60 to 90 GHz, one with a typical gain of 25 dBi and a HPBW of 10° , and one with a typical gain of 10 dBi and a HPBW of 55° .

The vehicle that was used for the channel measurements is a built-up cab (BUC), an adapted sport utility vehicle located inside the WMG 3xD Simulator at the University of Warwick [10]. The 3xD Simulator is housed inside a Faraday cage, and absorbing material on the walls and roof makes the room anechoic for radio frequency (RF) radiation with frequencies above 1.3 GHz. This RF shielding allows to emulate fully the highly complex and demanding signal environment that a vehicle encounters on a road. Moreover, it enables channel sounding in shielded and controlled automotive scenarios that are an important application area for mmWave technology. A mobile board, fitted with absorbing material, provided blockage of signal reflections from the experimental setup itself.

Our channel sounding equipment uses the pulse compression method and consists of an R&S SMW200A Vector Signal Generator, an R&S SMZ90 Frequency

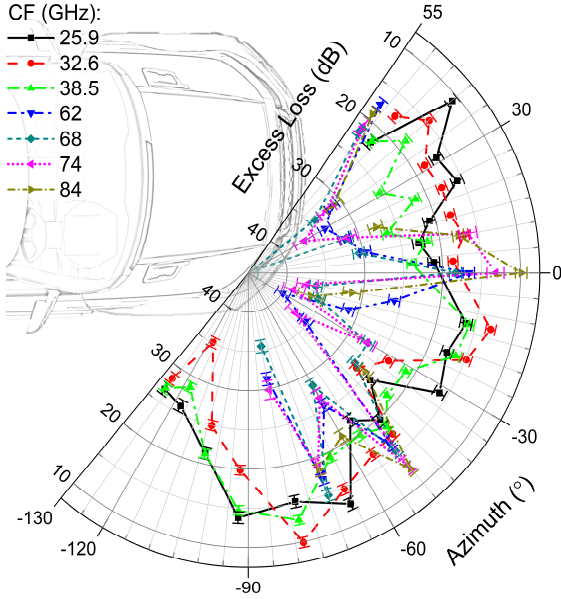


Fig. 2. Polar plot of the measured excess loss in the engine bay channel near the vehicular headlight. For various carrier frequencies (see legend), the EL is plotted versus the antenna pair orientation with the error bars indicating one standard deviation interval. The plot's origin is at the RX location in the engine bay and the lines connecting the measured values are guides to the eye.

Multiplier, an R&S FSW85 Signal and Spectrum Analyzer and an R&S RTO2044 Digital Oscilloscope. The former two devices enable the transmission of frequency band limited signals with a CF up to 90 GHz and an arbitrary modulated waveform with clock frequencies up to 2.4 GHz. The latter two devices enable the processing of the received signals with a maximum sampling rate of 2.4 GHz. The resulting I/Q data are forwarded to the R&S Channel Sounding Software, which autocorrelates the received I/Q data with the originally transmitted signal. The equipment is synchronized by means of direct, calibrated coaxial connections of their time reference and trigger channels. A 2 GHz bandwidth signal was generated and analyzed, providing a time resolution of 0.5 ns, equivalent to a spatial resolution of 15 cm. For this bandwidth, the numeric bit resolution of the setup's analog-to-digital converter is 10 bit, resulting in a 60 dBc dynamic range of the spectrum analyzer.

For CFs up to 40 GHz, a filtered Frank-Zadoff-Chu sequence [11] with a length of 120,000 samples was used as a channel sounding waveform, resulting in a channel impulse response (CIR) update rate of 50 μ s. Per antenna constellation 1024 CIR measurements were automatically triggered, and their results were stored, averaged and further analyzed. For CFs between 60 and 90 GHz, a custom Chirp sequence with a length of 480,000 samples was used; resulting in a CIR update rate of 200 μ s. 256 CIRs were measured for each antenna constellation.

IV. RESULTS AND DISCUSSION

As our interest lies in determining the excess path loss of the engine bay channel near the vehicular headlight, detailed calibration measurements have been carried out to determine the loss due to the equipment's components. Each previously described antenna pair was separated with incrementing distance, boresight aligned and the maximum received power and absolute time delay of the occurrence were determined.

$$PL_{FS}(d, f)[dB] = P_{TX} - P_{RX} + G_{TX}(f) + G_{RX}(f) - L_{TX}(f) - L_{RX}(f) - 20\log_{10}(4\pi df/c) \quad (1)$$

is Friis' free space transmission equation [12] for the antenna distance and frequency dependence of free space path loss, where PL_{FS} is the free space path loss at distance d for frequency f , P_{TX} and P_{RX} are the transmitter output and received power, G_{TX} and G_{RX} are the transmitter and receiver antenna gains, L_{TX} and L_{RX} are the transmitter and receiver losses, and c is the speed of light in vacuum. The excess loss is then defined as:

$$EL(f)[dB] = P_{RX} - \text{cal}(f) - 20\log_{10}(d) \quad (2)$$

where $\text{cal}(f)$ are the frequency and setup dependent calibration factors. When during the measurements a clear line of sight (LOS) signal is observed in a CIR, its relative delay is converted into a distance and used as d in (2). This minimizes the effect of small systematic errors in the exact antenna placement on d .

The root mean square delay spread of the determined power delay profiles (PDPs) is calculated following standard procedures [13]. We only take into account signals larger than our defined noise threshold, 6 dB above the measurement noise floor; based on the average power plus standard deviation of the final 20 % of the PDP-data, in which no MPCs are expected.

The polar plot in Fig. 2 displays the measured EL in the engine bay channel near the vehicular headlight for various antenna pair orientations, shown as the azimuth, and for the CFs of interest. RX is located at the plot's origin, enabling a straightforward interpretation of the direction-dependent loss of the channel. A clear trend difference can be distinguished between the EL measured using antenna pair 1 and pair 2, at CFs below, respectively, above 40 GHz. For the latter, a large EL is displayed for specific azimuth angles, e.g. at -30° and 30° , due to metallic reflectors within the vehicular headlight's housing. Whereas for the former, maximal EL is only observed at the azimuth boundaries of the measurement, where either the car's front or its aluminum coachwork blocks the RF signal. This observation is explained by the omnidirectionality of the RX used in pair 1, allowing for the detection of MPCs due to reflections within the engine bay. As our channel sounding setup's spatial resolution is 15 cm, any MPC that falls within this range around the expected LOS path centered at 120 cm, will be interpreted as being LOS. Hence the EL only increases significantly when the car's aluminum coachwork blocks both LOS and non-LOS (NLOS) paths. For CFs above 40 GHz, the narrow HPBW of the horn antennas of pair 2 reduces the possible MPCs close to the LOS path. Hence, in this case, the observed EL directly displays the LOS-absorption due to the materials used in the vehicle on the path between RX and TX.

As expected, because the setup's calibration measurements are included in (2), no frequency dependence can be recognized within the sets of measurement results with either antenna pair 1 or pair 2. Per azimuth, the variation of EL within such a set is mainly caused by minor antenna beam pattern variations with frequency, which allow for small differences in possible MPCs near the LOS path due to the car's exterior, which cannot be represented by the pure LOS calibration measurements.

The minimum EL in Fig. 2 is 10 dB and due to the car's

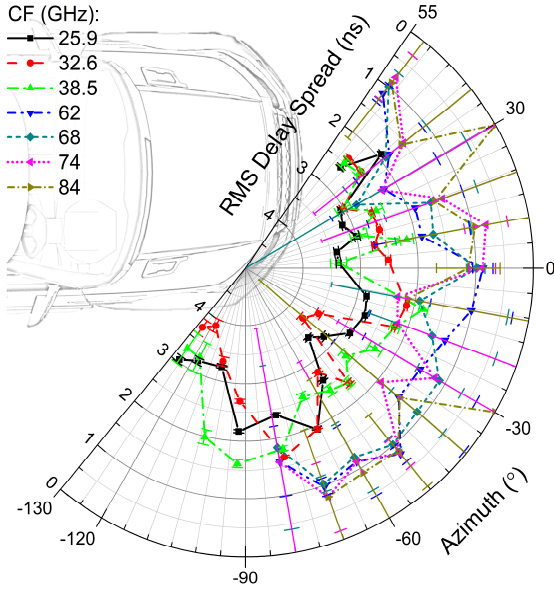


Fig. 3. Polar plot of the measured RMS delay spread in the engine bay channel near the vehicular headlight. For various CFs (see legend), the delay spread is plotted versus the antenna pair orientation with the error bars indicating one standard deviation interval. The plot's origin is at the RX location in the engine bay and the lines connecting the measured values are guides to the eye.

plastic front. Because this material is carbon fiber reinforced, the attenuation greatly exceeds values reported in literature, typically 4.3 dB per cm [14], and is considerably larger than 6.3 dB, the maximum EL measured inside an engine compartment for CFs up to 10.6 GHz [7]. This emphasizes the importance of channel sounding in realistic environments, which provide high-fidelity input into channel models, and demonstrates additionally, that the EL due to the car's exterior dominates the EL from the components inside the engine bay.

The polar plot in Fig. 3 displays the measured RMS-DS in the engine bay channel near the vehicular headlight for various azimuth, and for the CFs of interest. A clear difference is observed between the DS times determined using antenna pair 1 and pair 2, for CFs below, respectively, above 40 GHz, with the latter having much smaller absolute values. The explanation for this is twofold: firstly, the omnidirectional RX in pair 1 allows for the detection of more MPCs than the directional, narrow HPBW horn antenna in pair 2. Secondly, due to the setup and the frequency dependence of PL_{FS} in (1), the received power for CFs above 40 GHz is at least 10 dB smaller than for lower frequencies. Possible MPCs at longer delay times therefore have a higher probability to be below the setup's detection limit. This is also observed in the increased size of the standard deviation intervals for CFs above 40 GHz, reflecting that for particular, fixed antenna constellations, either very few or multiple weak MPCs can be recorded in consecutive PDPs.

In Fig. 3 the largest RMS-DS value is 4 ns, which is well below typical symbol lengths that are currently being discussed and implemented for mmWave communication; e.g. the IEEE 802.11ad Wi-Fi standard defines a subcarrier spacing of 5.15625 MHz for a CF of 60 GHz, which equals a symbol length of 194 ns. Therefore, our observed MPCs potentially cause narrowband symbol fading via interference, but only little time spreading and hence little intersymbol interference.

When comparing Fig. 2 and Fig. 3, e.g. from -90° to -130° , it is apparent that the RMS-DS increases with increasing EL. This is explained by the increased impact of MPCs on the RMS-DS when the LOS path is gradually blocked. However, for largest CF and EL, e.g. for 84 GHz at 30° and -30° , the RMS-DS approaches zero when only a single peak is detected in the PDP.

V. CONCLUSION

This Letter presents the typical EL and RMS-DS experienced in a mmWave communication channel near the vehicular headlight in an engine bay, which corner location provides a field of view of 140° . Measurements using an omnidirectional RX demonstrate that only few MPCs are present in this channel, resulting in a maximum DS time of 4 ns, and that for typical NLOS communication paths the signal is attenuated with 20 dB. Experiments including two directional horn antennas show that LOS communication can suffer from EL up to 35 dB. A comparison with channel sounding results within an engine bay [7] illustrates that this potential V2V mmWave communication channel is mostly affected by the car's exterior. Finally, since our measurements cover the frequency ranges for vehicular radar, the results additionally provide valuable information for the deployment of radar sensors within the engine bay.

VI. REFERENCES

- [1] T. S. Rappaport *et al.*, "Millimeter wave mobile communications for 5G cellular: It will work!," *IEEE Access*, vol. 1, pp. 335-349, 2013.
- [2] F. Boccardi, R. W. Heath, A. Lozano, T. L. Marzetta, and P. Popovski, "Five disruptive technology directions for 5G," *IEEE Commun. Mag.*, vol. 52, no. 2, pp. 74-80, Feb. 2014.
- [3] V. Va, T. Shimizu, G. Bansal, and R. W. Heath, *Millimeter wave vehicular communications: A survey*. Hanover, MA, USA: Now Foundations and Trends, 2015, vol. 10, no. 1, pp. 1-113.
- [4] P. Nikolic *et al.*, "Standards for 5G and beyond: Their use cases and applications," *IEEE 5G Tech Focus*, vol. 1, no. 2, 2017.
- [5] K. Mahler, W. Keusgen, F. Tufvesson, T. Zemen, and G. Caire, "Measurement-based wideband analysis of dynamic multipath propagation in vehicular communication scenarios," *IEEE Trans. Veh. Technol.*, vol. 66, no. 6, pp. 4657-4667, Jun. 2017.
- [6] P. Paschalidis *et al.*, "Investigation of MPC correlation and angular characteristics in the vehicular urban intersection channel using channel sounding and ray tracing," *IEEE Trans. Veh. Technol.*, vol. 65, no. 8, pp. 5874-5886, Aug. 2016.
- [7] U. Demir, C. U. Bas, and S. C. Ergen, "Engine compartment UWB channel model for intravehicular wireless sensor networks," *IEEE Trans. Veh. Technol.*, vol. 63, no. 6, pp. 2497-2505, Jul. 2014.
- [8] Resolution 238 (WRC-15), (2015). *Studies on frequency-related matters for International Mobile Telecommunications*. Available: www.itu.int/dms_pub/itu-r/oth/0c/0a/R0C0A00000C0014PDFE.pdf
- [9] J. Choi *et al.*, "Millimeter-wave vehicular communication to support massive automotive sensing," *IEEE Commun. Mag.*, vol. 54, no. 12, pp. 160-167, Dec. 2016.
- [10] S. Khatagir, S. Birrell, G. Dhadyalla, and P. Jennings, "Identifying a gap in existing validation methodologies for intelligent automotive systems: introducing the 3xD simulator," in *2015 IEEE Intelligent Vehicles Symposium (IV)*, Seoul, 2015, pp. 648-653.
- [11] R. L. Frank, S. A. Zadoff, and R. C. Heimiller, "Phase shift pulse codes with good periodic correlation properties," *IRE Trans. Inf. Theory*, vol. 8, no. 6, pp. 381-382, 1962.
- [12] H. T. Friis, "A note on a simple transmission formula," *Proc. IRE*, vol. 34, no. 5, pp. 254-256, 1946.
- [13] A. Goldsmith, "Statistical multipath channel models," in *Wireless Communications*, Cambridge, UK: CUP, 2005, p. 86.
- [14] T. W. Huang *et al.* (2009). *60 GHz transmission and reflection measurements*. Available: IEEE 802.11-09/0995r1